Journal of Wavelet Theory and Applications.
ISSN 0973-6336 Volume 1 Number 1 (2007), pp. 97–114

http://www.ripublication.com/jwta.htm

Wavelet Packet and TCQ Coding for SAR Raw Data Compression

Gowtham A. Tammana and Yuan F. Zheng
Department of Electrical and Computer Engineering,
The Ohio State University, Columbus, Ohio 43210
E-mail: {tammanag, zheng}@ece.osu.edu

Abstract

Synthetic aperture radar (SAR) is an imaging system which provides high resolution images of earth surface. The high resolution in the range direction is achieved by using large bandwidth signals and that in the azimuth direction is achieved by synthesizing a large aperture antenna using platform motion. The unique data collection geometry of SAR system requires that huge amounts of raw data be processed before obtaining a viewable image. Therefore, performing some form of compression on SAR raw data provides an attractive option for SAR systems. In this paper, we present a transform coding approach for SAR raw data compression. Due to presence of large dynamic range of frequency content in SAR raw data we propose the usage of wavelet packet transform. Furthermore, the transform coefficients are quantized using universal trellis coded quantizers. The quantization is performed independently on each subband in contrary to the current image coding algorithms like JPEG2000, considering the nature of SAR raw data where dependencies across scales are not evident. An adaptive rate allocation scheme is used to efficiently allocate the fixed rate resources among different subbands. Experimental results of the proposed method provides significant improvement in SNR results over standard block adaptive quantization (BAQ) and JPEG2000 techniques.

AMS Subject Classification: 78A25 Electromagnetic theory, general.
Keywords: Synthetic aperture radar, wavelet packet transform, trellis coded quantization, rate allocation.

1. Introduction

Synthetic aperture radar (SAR) is an imaging system which produces high resolution images of earth surface by using large bandwidth signals. The high resolution in the range direction is achieved by using large bandwidth signals while the high resolution

in the azimuth direction is achieved by synthesizing a large aperture using platform motion. SAR images are finding numerous applications in diverse areas like terrain mapping, cellular radio network planning, and target identification etc. The SAR data collection geometry requires that the received data has to be focussed before obtaining an image comprehensible to the human eye [6, 20]. A SAR system usually collects huge amount of data, and focusing of the raw data requires complex range varying phase compensation techniques which are generally performed off-board. The large amount of data generated have to be stored on-board or be transmitted to a ground station via a dedicated data link. Therefore, some form of compression on the raw data provides an attractive option for SAR systems.

A typical SAR system operates by transmitting signals of large bandwidth, usually linear frequency modulated (LFM) pulses, over a target area of interest and collects the reflections from the target. The reflected signal from a single point target is a complex weighted delayed version of the transmitted signal with delay being dependent on the distance between the target and the SAR platform. Assuming that the scatterers are distributed randomly over the target area then according to the central limit theorem, the statistics of the received signal can be modeled as Gaussian distribution with zero mean and slowly varying variance [11]. Because of this unique data acquisition SAR raw data does not exhibit the characteristics of natural optical images, which predominantly have low frequency spectrum and thus exhibiting strong correlation among adjacent samples. The high frequency content of SAR raw data is not negligible and has small correlation among adjacent samples. Due to these reasons, most optical image compression mechanisms do not translate well for SAR raw data.

Several researchers have proposed different methods for compressing SAR raw data [1, 5, 11, 13, 15, 17]. The most popular method is the *block adaptive quantization* (BAQ) [11]. BAQ is a simple non-uniform scalar quantizer whose quantizer levels are optimized to the local power fluctuations of the raw data. The local power fluctuations are captured by evaluating variance over the non-overlapping blocks of the raw data. The maximum block size is constrained by the fact that the signal power should be constant over the block and the minimum block size depends on the sufficient number of samples required for a proper Gaussian fit to the data. A 32x32 block size is usually employed and is found to be adequate [2, 11].

Quantizing the representation of a set of samples by a vector improves the compression performance and is the basic premise for vector quantization (VQ). VQ extensions of BAQ have been studied and were shown to improve the compression performance at the expense of computational complexity [13, 18]. Trellis coded quantization (TCQ) and its VQ counterpart techniques were studied in [17] to reduce the computational complexity of VQ designs. The results indicated improvement in compression performance with slight increase in computational complexities. The use of image transforms, fast Fourier transform (FFT) [2], discrete cosine transform [2] and wavelet packet transform (WPT) [19, 22] were also studied in the literature. In [4], a pre-processing technique, which was termed as range-focusing, is applied prior to quantizing the raw data with trellis coded vector quantization (TCVQ). The pre-processing operation was aimed to

bring correlation among the source samples, which is noise like, so as to exploit the advantages of TCVQ designs in the later stages of the compression algorithm. Even though the performance results were superior to BAQ the computational complexity is high for high bitrates.

Wavelet transform including WPT has been used to compress the SAR images by many authors in recent years [7, 9, 24]. The compression is on the processed SAR images, which are conceivable natural images, not the noise-like SAR raw data. It was pointed out that the SAR image contains speckle phenomena and using wavelet transform can combine both speckle-noise reduction and data compression [24]. Furthermore the SAR images have rich texture information; therefore, using WPT followed by TCQ performs better than the regular wavelet transform [9]. In [7], a new wavelet image coding technique called progressive space-frequency quantization is proposed to compress SAR images for the similar reasons as cited. We argue that SAR raw data have different characteristics from the regular SAR images. These characteristics must be carefully studied before proposing an effective compression algorithm. Unfortunately, compression of SAR raw data based on a thorough understanding of the characteristics of the data is under-represented in the literature.

In this paper we investigate the usage of wavelet transform and TCQ techniques for the compression of SAR raw data. Discrete wavelet transform (DWT) has been proven to be very successful for compressing optical images. SAR raw data possesses significant high frequency spectrum in contrast to the power spectrum of natural optical images which exhibits predominantly low frequency spectrum. Therefore, we use WPT, which performs uniform division of frequency spectrum, independently on real and imaginary parts of the complex SAR raw data. In [19], authors have used WPT along with scalar quantization for compressing SAR raw data. However, as we argue in the next section that energy compaction of wavelet packet transformation alone cannot provide good compression performances for SAR raw data. Therefore, in this paper instead of scalar quantization we propose to use trellis coded quantization techniques to quantize the subband coefficients. In addition, an adaptive bit allocation scheme is used to allocate the bits efficiently across the subbands. The performance of the proposed algorithm is evaluated by studying SNR results over the focussed SAR images. The results have indicated a significant improvement in performance over standard BAQ techniques with slight increase in computational complexity.

The rest of this paper is organized in the following manner. SAR data collection model is discussed first in Section 2. In Section 3, WPT is described and so is the main motivation for its usage in the current compression scheme. In Section 4, the trellis coded quantization (TCQ) is discussed followed by rate allocation strategy in Section 5. Finally the results of the proposed algorithm are presented in Section 6, which is followed by the conclusions in Section 7 of this paper.

2. SAR Data Collection Model

A typical SAR data collection geometry consists of transmitting large bandwidth signals over a target area of interest and recording the reflected returns. The high resolution

in the range direction, x domain, is obtained by using high bandwidth signals and the high resolution in the azimuth direction, y domain, is obtained by synthesizing a large antenna aperture using platform motion. Owing to the resolution constraints of a SAR system (bandwidth of the transmitted signal and length of the synthetic aperture), it is reasonable to assume the presence of a large number of individual scatterers within a resolution cell. Therefore, each scatterer contributes a phase and magnitude change to the backscattered signal of the corresponding resolution cell:

$$\chi(x, y) \exp(j\phi(x, y)) = \sum_k \chi_k(x, y) \exp(j\phi_k(x, y)) \tag{2.1}$$

where $\chi_k(x, y)$ and $\phi_k(x, y)$ are the magnitude and phase response of the individual scatterers in a single resolution cell corresponding to location (x, y). The phase returns $\phi(x, y)$ can be modeled as uniformly distributed random variable in $[-\pi, \pi]$, since the phase due to different scatterers within a resolution cell differ considerably due to the large range distances. Under the presence of a number of scatterers assumption, the real and imaginary parts of the received signal can be modeled as zero-mean Gaussian distributed random variables, by the central limit theorem, with slowly varying variance due to changes in the antenna spectrum.

It can be seen from (2.1) that the target area function has a highly random phase function, which indicates that the Fourier spectrum is very broad and extends in the entire bandwidth of the SAR system. Because of this high frequency content of the target image, the received data which is convolution of transmitted signal with the target function exhibits much noise like characteristics (this noise like characteristics referred as *speckle* is exploited efficiently in SAR interferometry) and due to which SAR raw data exhibits very little spatial correlation than the natural optical images.

Several SAR raw data compression approaches perform SAR raw data compression using adaptive scalar [1, 2, 11] and vector quantization [2, 13, 15] techniques. These techniques provide reasonably good compression performances due to the fact that the raw data exhibits very low spatial correlation among its pixels. In this paper, we use transform coding approach to compress SAR raw data. Transform approaches have been widely used for regular optical image compression and have achieved impressive results [3, 8, 14]. It has been shown that transform approaches are particularly powerful in exploring correlations among pixels in the frequency domain. The same approaches may lead to improved results in compressing SAR raw data by effectively exploring any possible correlation among the pixels of the SAR raw data. However, since the distribution of the SAR raw data demonstrates its unique feature as just discussed, transform approaches as used in optical image compression cannot be directly employed. Instead, we propose the use of WPT which has a uniformly decimated filter bank structure as opposed to dyadic wavelet transform. The advantages and applications of WPT will be discussed in the next section.

3. Wavelet Transform

In this section, we provide a brief description on wavelet transform and interested readers are referred to [23] for more details. Using discrete wavelet transform (DWT) a signal can be represented in an orthonormal basis, $\{\psi_{k,n}; k, n \in \mathbb{Z}\}$, consisting of countably-infinite set of wavelets. DWT representation of a zero-mean random vector X can be written as

$$X = \sum_{k,n} d_k[n]\psi_{k,n} \tag{3.1}$$

$$d_k[n] = \langle \psi_{k,n}, X \rangle \tag{3.2}$$

where $\{d_k[n] : k, n \in \mathbb{Z}\}$ are wavelet coefficients. The most significant feature of wavelet transform is that the countably-infinite set of wavelets $\{\psi_{k,n}(t) = 2^{-k/2}\psi\left(2^{-k}t - n\right); k, n \in \mathbb{Z}\}$ are produced by translations and dilations of a single mother wavelet, $\psi(t)$. Scaling functions $\{\varphi_{k,n}; k, n \in \mathbb{Z}\}$, which are also produced by translations and dilations of a single mother scaling function $\varphi(t)$, can be used to approximate the signal upto a particular level of detail [23]. An L-level wavelet decomposition of a signal can be written as

$$x(t) = \sum_{n} a_L[n]\varphi_{L,n}(t) + \sum_{l=1}^{L}\sum_{n} d_l[n]\psi_{l,n}(t) \tag{3.3}$$

where $a_L[\cdot]$ and $d_l[\cdot]$ represent the approximation and detail coefficients of the signal, respectively. In practice, discrete wavelet transform of a signal is calculated by fast algorithm using a set of filter coefficients $h[\cdot]$ and $g[\cdot]$ determined by scaling equations [23]. Such a finite one-dimensional (1-D) DWT decomposition structure is shown in Fig. 1, where $H(z)$ and $G(z)$ are scaling and wavelet filters, respectively. In the filter bank terminology the structure in Fig. 1 is known as hierarchical filter bank with $H(z)$ and $G(z)$ as low-pass filter and high-pass filter, respectively. Therefore, in the filter bank view point each level of decomposition can be seen as information content in a particular frequency band (subband) of the original signal spectrum. Due to the hierarchical division of the frequency spectrum the bandwidth of successive subbands increase to the powers of two. 1-D DWT structure can be extended to evaluate separable two-dimensional (2-D) wavelet transform of a 2-D signal, e.g., image, by using 1-D wavelet filters along both horizontal and vertical dimensions (see Fig. 2 for a two level DWT).

The discrete wavelet transform has been proven to be very successful for compressing optical images. One of the several reasons for its success can be attributed to the structure of power spectrum which falls off exponentially for optical images (see Fig. 3). This structure makes the use of dyadic wavelet transform structure very efficient for compressing the optical images, since it provides good frequency selectivity for achieving substantial coding gain [21]. Following in the above lines of frequency spectrum perspective, SAR raw data frequency spectrum has to be studied for better utilization of wavelet properties.

Power spectral density (PSD) of SAR raw data can be derived from the power normalized raw data using standard spectral estimation methods. The power normalization

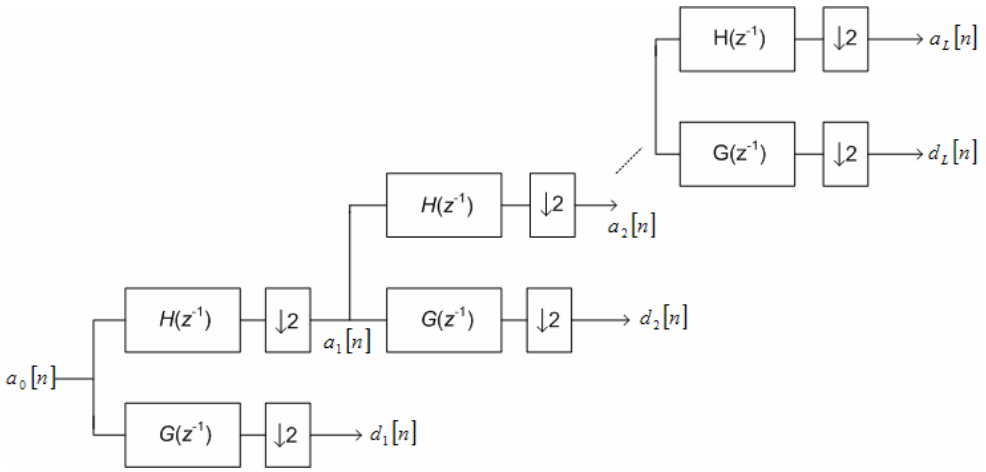

Figure 1: Filter-bank structure of discrete wavelet transform

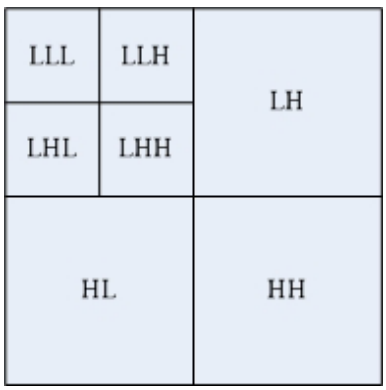

Figure 2: A two level 2-D DWT of an image; L and H indicate low and high frequency regions

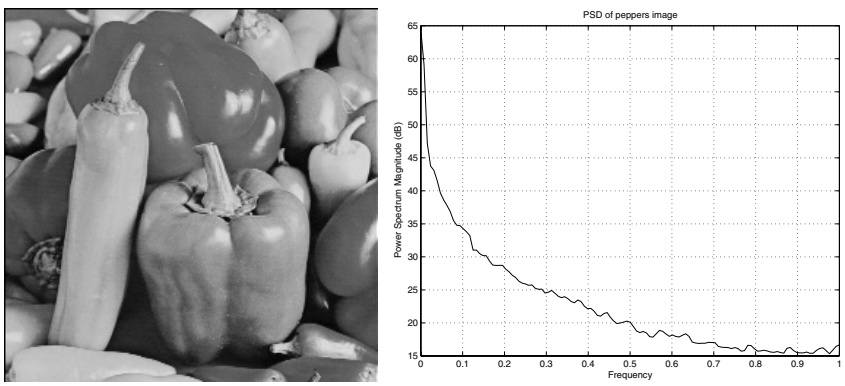

Figure 3: The image on left is a standard optical test image, and its power spectrum is shown in rightside of the figure

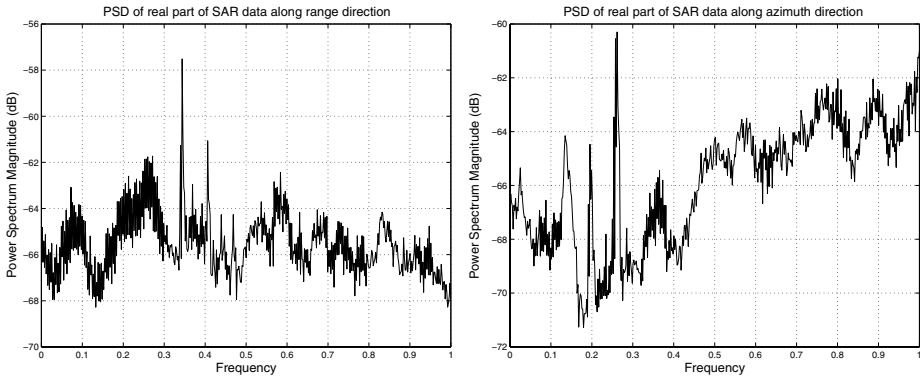

Figure 4: The left plot shows the normalized power spectrum of the real part of the SAR raw data, used in our experiments, along the range direction and the right plot shows the normalized power spectrum of the real part of the SAR raw data along the azimuth direction

of the data is done so as to ensure the stationarity of the data. Fig. 4 shows PSD of raw data using Welsh's averaged periodogram method along both range and azimuth directions.

The power spectrum of SAR raw data indicates a significant high frequency spectrum, which means that a lot of significant coefficients remain in high frequency regions after DWT. In the case of optical images, the number of significant coefficients in high frequency regions are much less and is translated in the small variance of high frequency subbands. Because of this smaller variance of the high frequency bands high compression performances can be achieved by using less number of bits for those regions and are completely ignored for very low bit rates. In contrast, as indicated in Fig. 4 power spectrum of SAR raw data has shown a large dynamic range in the frequency spectrum. Therefore, the use of DWT structure will not provide good frequency selectivity for achieving optimal coding gain. Because of the high frequency content of SAR raw data, WPT is used in this work. By WPT we refer to the scheme where all the high frequency components in Fig. 1 are further decomposed into low and high frequency regions, which can be pictorially represented by Fig. 5 and Fig. 6.

The WPT structure divides the power spectrum into regions of equal bandwidths. This uniform division of frequency spectrum by WPT better facilitates the capturing of the frequency content of the raw data. Therefore, in this paper we use wavelet packet transform for compressing SAR raw data.

4. Trellis Coded Quantization

The amount of correlation present in the SAR raw data is limited and transformation of the signal in the wavelet basis alone cannot provide good compression performances. An efficient quantization procedure whose rate-distortion (R-D) characteristics are close to

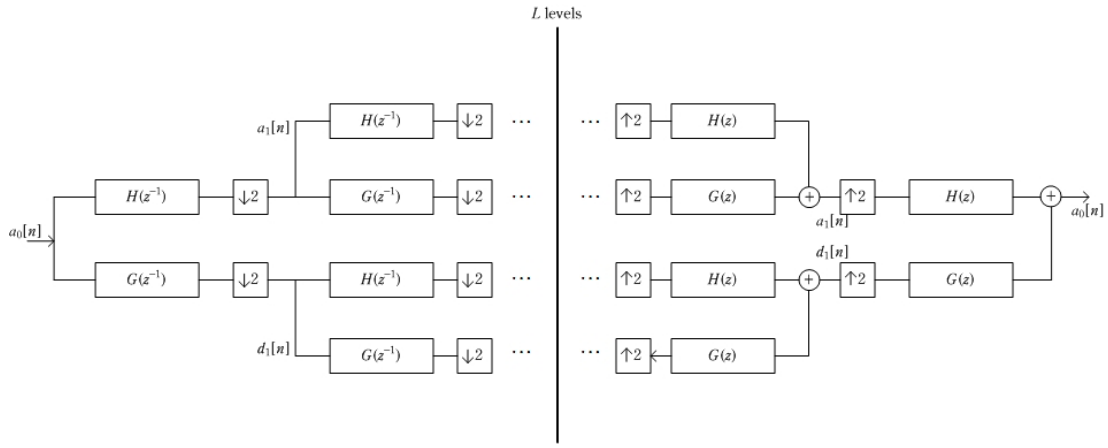

Figure 5: Block diagram representation of the wavelet packet transform

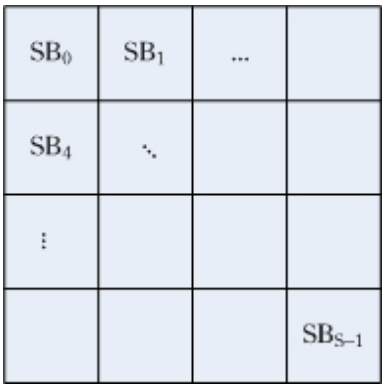

Figure 6: A 2-level WPT representation of an image; SB denotes subband and S denotes the total number of subbands

the R-D curve of Gaussian distribution is needed. In this paper, trellis coded quantization (TCQ) procedure is used for this purpose.

TCQ lies, in terms of advantages, somewhere in between scalar quantization (SQ) and VQ. SQ is a simple comparison procedure with minimal computational complexity and with reasonably good R-D performance. VQ, a straight forward extension of SQ, quantizes a K-dimensional vector, representing a set of samples instead of a single sample. VQ provides good R-D performance at the expense of increased computational complexity. The advantage comes from optimal partitioning of the K-dimensional sample space. The codebook size and complexity increases exponentially with increase in vector dimensions. TCQ on the other hand provides R-D performance close to that of VQ design but with relatively low complexity. The computational complexity of TCQ encoding operation is of the order $O(PN)$, where P is the size of the trellis and N is the number of source samples to be quantized. To keep the computational complexity of

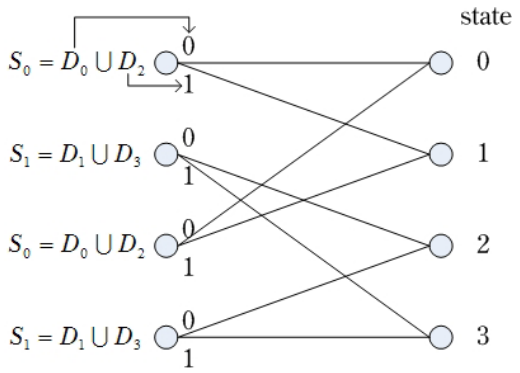

Figure 7: 4-state trellis diagram

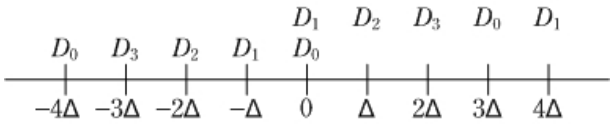

Figure 8: UTCQ codebook configuration

the algorithm under check we chose to use a 4-state trellis diagram in the TCQ encoding algorithm.

TCQ can be thought of as a scalar quantizer with memory, where the current source sample is quantized by a codebook depending on the previously quantized source sample. The choice of a particular codebook is determined by the previously quantized source sample and is done with the help of a P-state trellis diagram (see Fig. 7) defined by a rate-$\frac{1}{2}$ convolutional encoder. In this section, we briefly discuss the operation of a TCQ quantizer, in particular universal TCQ (UTCQ) configuration, and more details can be found in [12, 16].

Assume that N samples, from a memoryless source X, $\{X_1, X_2, \ldots, X_N\}$ are to be encoded using a uniformly quantized codeset $\mathcal{C}$ with step size Δ and consisting of $J+1$ elements. The codeset is divided into two codebooks S_0 and S_1 known as supersets each consisting of subsets (D_0, D_2) and (D_1, D_3), respectively (see Fig. 8). Each state in the trellis is assigned its own codebook to use and the choice of the subset determines the next state correspondingly which codebook to use for the next sample. The quantized source sample can be represented by codeword $s_i(j)$, representing jth codeword from superset S_i:

$$s_i(j) = \begin{cases} 2j + i - 1, & j = 1, \ldots, \frac{J}{4} \\ 0, & j = 0 \\ 2j + i, & j = -\frac{J}{4}, \ldots, -1 \end{cases} \tag{4.1}$$

for $i = 0, 1$.

4.1. Encoder

A source sample at state 0 can only use codewords from codebook S_0 and the choice of subset in S_0 determines the next state in the trellis path and correspondingly which codebook to use for the next source sample. To encode N samples of X, N such stages are cascaded and the TCQ algorithm finds $\hat{X}_{n_i}$,which denotes a codeword from superset S_i closest to X_n, for $1 \leq n \leq N$ and $0 \leq i \leq 1$:

$$\hat{X}_{n_i} \in \{s_i(j), -\frac{J}{4} \leq j \leq \frac{J}{4}\} \tag{4.2}$$

where $s_i(j)$ denotes the j^{th} codeword from superset S_i. The final quantized source, $\hat{X}$, which minimizes the mean square distortion D is found by *Viterbi* algorithm:

$$D = \sum_{n=1}^{M} \left(X - \hat{X}_n\right)^2 \tag{4.3}$$

where

$$\hat{X}_n \in \{\hat{X}_{n_i}, 0 \leq i \leq 1\}. \tag{4.4}$$

If $J + 1 = 2^R$, then R bits are necessary to represent a codeword in codeset $\mathcal{C}$ using a standard uniform scalar quantization procedure. In TCQ, a particular source sample is encoded using codewords from one of the supersets S_0 and S_1. Therefore, $R - 1$ bits are sufficient to represent a codeword from one of the supersets. The selection of superset can be unambiguously decoded by following the trellis path in the trellis diagram. Hence, in total $R - 1$ bits are sufficient for encoding the source using a codebook consisting of 2^R codewords. For a more detailed description of TCQ coding the readers are referred to [12, 16]. The TCQ output indices can be entropy coded to further compress the output stream, and a scheme proposed in [10] is used in this paper.

4.2. Decoder

The $R - 1$ bit symbol is decoded into $s_i(j)$ representing the jth codeword from the ith superset. The usage of $s_i(j)$ as reconstruction levels is not optimal in the mean square distortion sense. For optimal MSE the centroid of source samples which are quantized to $s_i(j)$ should be used. In general, it is quite difficult to analytically formulate the optimal reconstruction levels, and they are usually estimated from training data. In the present case, the optimal reconstruction values can be evaluated for Gaussian distribution, as raw data is modeled as Gaussian, and the same can be used at the decoder.

4.3. Significance Test and TCQ

In an attempt to reduce the computational cost of TCQ we investigated the use of significance test in the TCQ operation. Since each subband is Gaussian the zero-bin in the codeset $\mathcal{C}$ has the highest probability of selection, i.e., most of the samples are encoded to

Table 1: Comparison of SNR performance (in dB) of various encoders for zero-mean Gaussian source with unit variance for various bitrates.

Coding Technique	Rate in bits/sample					
	0.50	1.00	1.50	2.00	2.50	3.00
BAQ		4.40		8.70		14.00
dead-zone	2.13	4.61	7.17	10.16	13.38	16.47
Significance test + TCQ	2.18	4.70	7.41	10.45	13.72	16.89
TCQ	2.21	4.91	7.45	10.70	14.03	17.17
UTCQ	2.34	5.02	8.05	11.17	14.25	17.31

zero. Therefore, a significance map $I_s[.]$ is used to differentiate significant coefficients from coefficients near the zero region:

$$I_s[p] = \begin{cases} 1, & |d_s[p]| > \tau \\ 0, & \text{o.w} \end{cases} \tag{4.5}$$

where $d_s[.]$ are coefficients of subband s and τ is some threshold.

The significant coefficients are then quantized using UTCQ encoding scheme with an offset $\pm\tau$ for the codewords. The SNR results for encoding a Matlab generated independent and identically distributed unit variance Gaussian source using this encoder are shown in Table 1.

One of the main reasons for Significance test + TCQ schemes underperformance is because of the large offset τ in the new codebook. In the UTCQ configuration, the codewords in supersets S_0 and S_1 are asymmetric with respect to zero codeword and this facilitates optimal sign reversal for some of the source samples, and since majority of the source samples are around this region it brings in substantial decrease in mean square error. Similar sign reversal is catastrophic, in terms of mean square error, for the modified codebook configuration and hence is the major reason for its under performance compared to the UTCQ coding scheme.

5. Rate Allocation

The WPT operation on SAR raw data produces in general subbands of different variances. For optimal compression it is necessary to optimally allocate the fixed rate resource among different subbands. In general, it is very difficult to express UTCQ R-D performance analytically. Therefore, we adopt high rate approximations to model UTCQ distortion performance for efficient allocation of rates to the subbands. Under high rate approximation the distortion versus rates assigned to the subbands can be modeled as [21]:

$$D(R) = \sum_{s=0}^{S-1} \beta_s \gamma_s \sigma_s^2 D_s(R_s) \tag{5.1}$$

with

$$D_s(R_s) = \varepsilon_s^2 2^{-2R_s} \tag{5.2}$$

where $D_s(R_s)$ is the high rate approximation of UTCQ rate-distortion curve for unit variance Gaussian source, S is the total number of subbands, σ_s^2 is the variance of subband s, and the parameters β_s and γ_s represent the fraction of coefficients in subband s and filter energies. An appropriate value for ε_s^2 was chosen by fitting the distortion model curve of (5.1) to the actual UTCQ R-D curve. It is worthwhile to point that the above mentioned model is not accurate for low bit rates, but is adequate for SAR raw data compression since good distortion performances are only observed for high bit rates; interested readers are pointed to [12] for modeling at low bit rates.

The objective of the rate allocation is to minimize the overall distortion in the image subject to the rate constraint, $R \leq R_0$:

$$R = \sum_{s=0}^{S-1} \beta_s R_s. \tag{5.3}$$

This problem can be solved by minimizing the following Lagrangian functional [21]:

$$J = \sum_{s=0}^{S-1} \beta_s \gamma_s \sigma_s^2 D_s(R_s) + \lambda \sum_{s=0}^{S-1} \beta_s R_s. \tag{5.4}$$

For orthonormal full wavelet packet decomposition γ_s and β_s can be replaced by 1 and $\frac{1}{S}$, respectively. Differentiating (5.4) with respect to R_s, we obtain

$$D_s'(R_s) = -\frac{\lambda}{\sigma_s^2}. \tag{5.5}$$

After a series of algebraic manipulations, it can be proved that the individual rates are given by

$$R_s = R + \frac{1}{2}\log_2 \frac{\varepsilon_s^2 \sigma_s^2}{\prod_{j=0}^{S-1} (\varepsilon_j^2 \sigma_j^2)^{1/S}}. \tag{5.6}$$

The above rate allocation ensures that all D_is are equal and the average distortion is given by

$$D = \left(\prod_{s=0}^{S-1} \varepsilon_s^2 \sigma_s^2 \right)^{\frac{1}{S}} 2^{-2R}. \tag{5.7}$$

The rate allocation in (5.6) is used in our algorithm. In some cases, some of the R_ss turn out to be negative in which case the corresponding subbands are given zero rate and the rate allocation is recomputed on the remaining subbands.

6. Experimental Results

The proposed algorithm is evaluated on a set of simulated SAR raw data of dimensions 412x412. The performance is evaluated using SNR criteria on the final focussed SAR image (see Fig. 9) since this is of major interest in most applications and is defined as

$$SNR = 10\log_{10}\frac{\|\mathbf{x}\|^2}{\left\|\mathbf{x} - \frac{\|\mathbf{x}\|}{\|\hat{\mathbf{x}}\|}\hat{\mathbf{x}}\right\|^2} \tag{6.1}$$

where $\mathbf{x}$ represents the focused image obtained from uncompressed raw data and $\hat{\mathbf{x}}$ represents the focused image obtained from compressed raw data. The power normalization is performed on the compressed image to ensure same power as in the original image since quantization operation in general is not a power conserving operation. The required wavelet coefficients are generated by 3-level wavelet packet decomposition using orthonormal Daubechies-4 wavelet basis [23]. As in the block size choice of BAQ, the number of levels of WPT is restricted such that an individual subband has sufficient number of samples for obtaining a proper estimate of the variance of subband. We observed that usually a 3-level WPT is sufficient and further increase in levels will increase the overhead information required to store the variance information of subbands without significant increase in compression performance. TCQ encoder using 4-state trellis diagram is used to quantize the wavelet coefficients. The quantization is performed independently on the subband coefficients with step sizes as determined by adaptive rate allocation algorithm. The computational complexity of the proposed algorithm is moderate. The main sources of computational complexities are WPT, TCQ and arithmetic coding following the TCQ and they are of order $O(N^2\log(N))$, $O(4N^2)$, and $O(\max(N^2, RN^2))$, respectively for NxN SAR raw data dimensions.

The results of the proposed algorithm for the test data set are tabulated in Table 2 along with performances of standard BAQ, JPEG2000 and scheme presented in [19]. The results indicate that for all bit rates the proposed technique resulted in significant improvement over the other techniques. The results for BAQ algorithm are obtained by using Lloyd- Max quantizer on non-overlapping blocks of size 32x32. The superiority over BAQ can be attributed to the coding gain of WPT and efficient rate allocation. The results for WPT+dead-zone method were generated as described in [19] with some minor modifications. In [19] the reconstruction levels in decoder are obtained by scaling the decoded index by a fixed amount and adding some fixed offset. The scaling and offset values are fixed for all the decoded indices. In general it is sub-optimal to use same reconstruction levels at encoder as well as decoder. Here, we present the results using optimal reconstruction levels which were generated in decoder by using Gaussian training samples. The major reason for improvement over [19] is due to the use of the UTCQ encoding procedure which offers better performances for Gaussian sources than dead-zone quantizer.

The results for JPEG2000 were obtained by using the JPEG2000 software provided at www. kakadusoftware.com. For comparison purposes we considered the options of single tile and single quality layer for JPEG2000 algorithm. The focussed images for

Table 2: SNR performance (in dB) for all the techniques considered at different bit rates. Proposed technique, BAQ, JPEG2000 and technique in [19]

Bit rate	BAQ	WPT+UTCQ	JPEG2000	WPT+dead-zone [19]
0.50	–	5.62	4.13	5.37
1.00	7.11	8.56	7.08	8.04
1.50	–	11.81	9.12	11.12
2.00	12.31	15.02	12.05	13.87

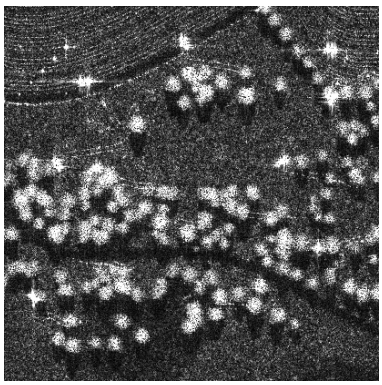

Figure 9: Uncompressed focused SAR image

the proposed technique and JPEG2000 are shown in Fig. 10 and Fig. 11, respectively. It is evident in the images that there is an increase in the overall noise floor in the focussed images obtained by JPEG2000 and this may affect any post-processing methods that might be applied on the focussed SAR images. We believe that the use of DWT structure instead of WPT is one of the main reason for lower performance of JPEG2000. The other significant reason is due to the fact that the efficiency of EBCOT encoding engine in JPEG2000 depends on the effective probability models of pixels which are highly influenced by adjacent pixel dependencies in subbands which are often very rare in SAR raw data. The results prove that WPT is more suitable for compressing SAR raw data than DWT because of the high frequency contents in the power spectrum of the SAR raw data.

7. Conclusions

We have described a new approach for compressing SAR raw data. The goal is to deliver better performance than that of existing methods. We explored the use of wavelet transform based methods, particularly WPT for the purpose. We analyzed the feature of the SAR signals and revealed the large dynamic range of the frequency content of the SAR raw data in contrast to that of regular optical images. Based on the analysis,

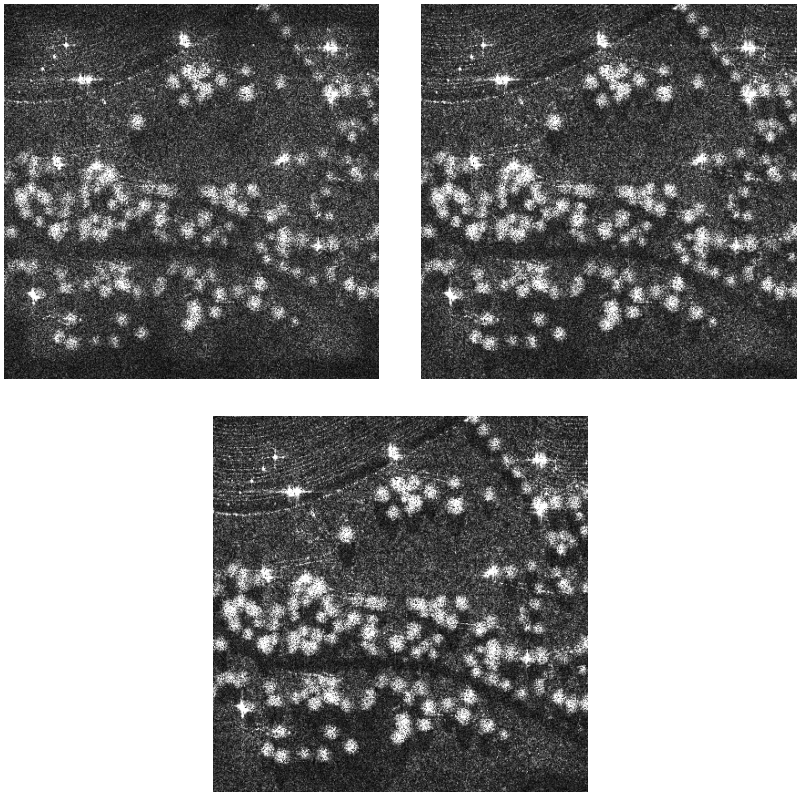

Figure 10: Compressed SAR images using proposed method at the following rates: (a) 1.0 bits/sample; (b) 1.5 bits/sample; (c) 2.0 bits/sample

we argued that a uniformly decimated wavelet transform structure is better suited for SAR raw data compression, thus the WPT method. To further push the performance to the limit, we have proposed that the subband coefficients be quantized using rate controlled UTCQ encoder since the latter has a close rate-distortion characteristics to that of Gaussian distribution. A 4-state trellis coded approach is used in UTCQ encoder design to keep computational complexity under check. We have also explored the use of significance test in UTCQ encoding operation and found that if sign information of wavelet coefficients can be encoded efficiently, then it can substantially decrease the computational complexity of UTCQ for low bit rates. The computational complexity of the proposed algorithm is moderate and is independent of the target bit rate. Again for pushing the performance even further, we presented an adaptive rate allocation method for allocating the fixed bit rate resource among different subbands based on Lagrangian optimization to minimize distortion. The experimental results of the proposed algorithm were shown to provide significant improvement of about 1.3–3.0 dB over standard BAQ and JPEG2000 techniques.

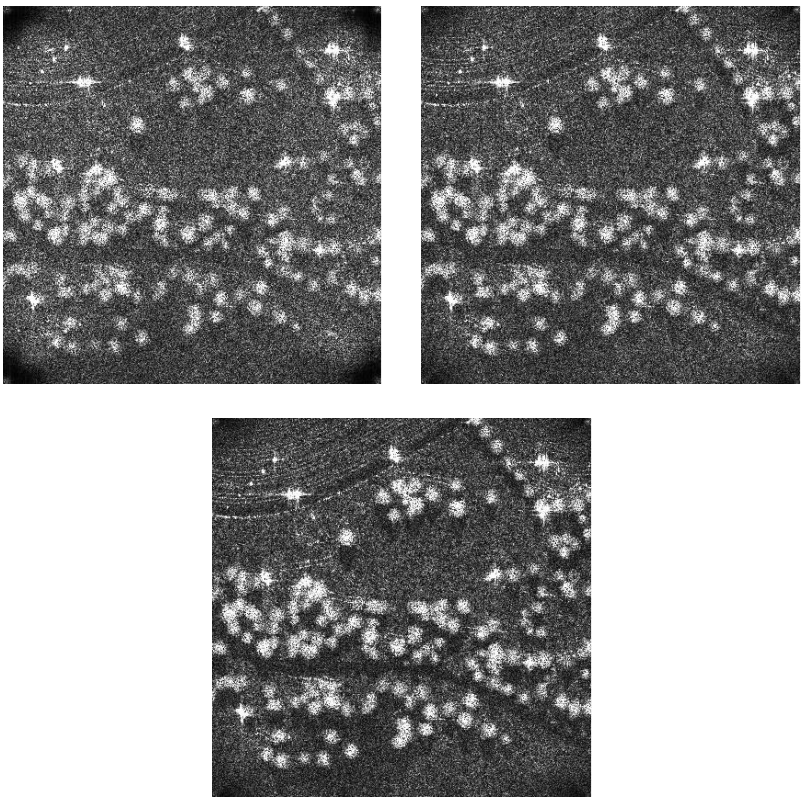

Figure 11: Compressed SAR images using JPEG2000 at the following rates: (a) 1.0 bits/sample; (b) 1.5 bits/sample; (c) 2.0 bits/sample

References

[1] Algra T., 2000, Compression of Raw SAR Data Using Entropy-constrained Quantization, Proc. IGARSS, 6, pp. 2660–2662.

[2] Benz U., Strodl K., and Moreira A., 1995, A Comparison of Several Algorithms for SAR Raw Data Compression, IEEE Transactions on Geoscience and Remote Sensing, 33(5), pp. 1266–1276.

[3] Chen Y. and Pearlman W., 1996, Three-dimensional Subband Coding of Video Using the Zerotree Methods, Proc. SPIE Visual Communications and Image Processing, 2727, pp. 1302–1312.

[4] D'Elia C., Poggi G., and Verdoliva L., 2001, Compression of SAR Data Through Range Focusing and Variable-Rate Trellis Coded Quantization, IEEE Transactions on Image Processing, 10(9), pp. 1278–1287.

[5] Fischer J., Benz U., and Moreira A., 1999, Efficient SAR Raw Data Compression in Frequency Domain, Proc. IGARSS, 4, pp. 2261–2263.

[6] Gough P. and Hawkins D., 1997, Unified Framework for Modern Synthetic Aperture Imaging Algorithms, Int. Jour. Imaging Syst. Technology, 8(4), pp. 343–358.

[7] Gleich D., Planinsic P., Gergic B., and Cucej Z., 2002, Progressive Space Frequency Quantization for SAR Data Compression, IEEE Transactions on Geoscience and Remote Sensing, 40(1), pp. 3–10.

[8] He C., Dong J., Zheng Y.F., and Gao Z., 2003, Optimal 3-D Coefficient Tree Structure for 3-D Wavelet Video Coding, IEEE Transactions on Circuits and Systems for Video Technology, 13(12), pp. 961–972.

[9] Xingsong Hou, Guizhong Liu, and Yiyang Zou, 2004, SAR Image Data Compression Using Wavelet Packet Transform and Universal-Trellis Coded Quantization, IEEE Transactions on Geoscience and Remote Sensing, 42(11), pp. 2632–2641.

[10] Joshi R.L., Crump V.J., and Fischer T.R., 1995, Image Subband Coding using Arithmetic Coded Trellis Coded Quantization, IEEE Transactions on Circuits and Systems for Video Technology, 5(6), pp. 512–523.

[11] Kwok R. and Johnson W.T.K., 1989, Block Adaptive Quantization of Magellan SAR Data, IEEE Transactions on Geoscience and Remote Sensing, 27(4), pp. 375–383.

[12] Kasner J.H., Marcellin M.W., and Hunt B.R., 1999, Universal Trellis Coded Quantization, IEEE Transactions on Image Processing, 8(12), pp. 1677–1687.

[13] Lebedeff D., Mathieu P., Barlaud M., Lambert-Nebout C., and Bellemain P., 1995, Adaptive Vector Quantization for Raw SAR Data, Proc. IEEE Int. Conf. Acoustics, Speech, Signal Processing'95, 4, pp. 2511–2514.

[14] Lin C., Zhang B., and Zheng Y.F., 2000, Packed Integer Wavelet Transform Constructed by Lifting Scheme, IEEE Transactions on Circuits and Systems for Video Technology, 10(8), pp. 1496–1501.

[15] Moreira A. and Blaeser F., 1993, Fusion of Block Adaptive and Vector Quantizer for Efficient SAR Data Compression, Proc. IGARSS, 4, pp. 1583–1585.

[16] Marcellin M.W. and Fischer T.R., 1990, Trellis Coded Quantization of Memoryless and Gauss-Markov Process, IEEE Transactions on Communications, 38(1), pp. 82–93.

[17] Owens J.W., Marcellin M.W., Hunt B.R., and Kleine M., 1999, Compression of Synthetic Aperture Radar Video Phase History Data using Trellis-Coded Quantization Techniques, IEEE Transactions on Geoscience and Remote Sensing, 37(2), pp. 1080–1085.

[18] Poggi G., Ragozini A.R.P., and Verdoliva L., 2000, Compression of SAR Data Through Range Focusing and Variable-Rate Vector Quantization, IEEE Transactions on Geoscience and Remote Sensing, 38(3), pp. 1282–1289.

[19] Pascazio V. and Schirinzi G., 2003, SAR Raw Data Compression by Subband Coding, IEEE Transactions on Geoscience and Remote Sensing, 41(5), pp. 964–976.

[20] Soumekh M., 1999, Synthetic Aperture Radar Signal Processing, New York: Wiley.

[21] Taubman D.S. and Marcellin M.W., 2002, JPEG2000: Image Compression Fundamentals, Standards and Practice, Kluwer Academic Publishers.

[22] Tammana G.A., Zheng Y.F., and Ewing R.L., 2005, Synthetic Aperture Radar Raw Data Compression Using Wavelet Packet Transform and Trellis Coded Quantization, Proc. of IEEE Mid-west Symposium on Circuits and Systems, pp. 1705–1708.

[23] Vetterli M. and Kovacevic J., 1995, Wavelets and Subband Coding, Prentice-Hall.

[24] Zhaohui Zeng and Cumming I.G., 2001, SAR Image Data Compression Using a Tree-structured Wavelet Transform, IEEE Transactions on Geoscience and Remote Sensing, 39(3), pp. 546–552.